Technology in Cancer Research & Treatment
Volume 21: 1-15

DOI: 10.1177/15330338211067911
journals.sagepub.com/home/tct
SAGE

Alternative Splicing: A New Therapeutic Target for Ovarian Cancer

Shijie Yao, MM[1,2,3], Cheng Yuan, MD[1,2,3], Yuying Shi, MD[1,2,3], Yuwen Qi, MD[1,2,3], Radhakrishnan Sridha, MD[4], Mengyuan Dai, MD[1,2,3], and Hongbing Cai, MD[1,2,3]

Abstract

Background: Increasing evidences have shown that abnormal alternative splicing (AS) events are closely related to the prognosis of various tumors. However, the role of AS in ovarian cancer (OV) is poorly understood. This study aims to explore the correlation between AS and the prognosis of OV and establish a prognostic model for OV. **Methods:** We downloaded the RNA-seq data of OV from The Cancer Genome Atlas databases and assessed cancer-specific AS through the SpliceSeq software. Then systemically investigated the overall survival (OS)-related AS and splicing factors (SFs) by bioinformatics analysis. The nomogram was established based on the clinical information, and the clinical practicability of the nomogram was verified through the calibration curve. Finally, a splicing correlation network was constructed to reveal the relationship between OS-related AS and SFs. **Results:** A total of 48,049 AS events were detected from 10,582 genes, of which 1523 were significantly associated with OS. The area under the curve of the final prediction model was 0.785, 0.681, and 0.781 in 1, 3, and 5 years, respectively. Moreover, the nomogram showed high calibration and discrimination in OV patients. Spearman correlation analysis was used to determine 8 SFs significantly related to survival, including major facilitator superfamily domain containing 11, synaptotagmin binding cytoplasmic RNA interacting protein, DEAH-box helicase 35, CWC15, integrator complex subunit 1, LUC7 like 2, cell cycle and apoptosis regulator 1, and heterogeneous nuclear ribonucleoprotein A2/B1. **Conclusion:** This study provides a prognostic model related to AS in OV, and constructs an AS-clinicopathological nomogram, which provides the possibility to predict the long-term prognosis of OV patients. We have explored the wealth of RNA splicing networks and regulation patterns related to the prognosis of OV, which provides a large number of biomarkers and potential targets for the treatment of OV. Put forward the potential possibility of interfering with the AS of OV in the comprehensive treatment of OV.

Keywords

prediction models, alternative splicing, targeted therapy, ovarian cancer, splicing factor, nomogram

Abbreviations

AA, acceptor site; AD, alternate donor site; AP, alternate promoter; AS, alternative splicing; AT, alternate terminator; AUC, area under the curve; CAR, constitutive androstane receptor; CCAR1, cell cycle and apoptosis regulator 1; CDK12, cyclin-dependent kinase 12; DHX35, DEAH-box helicase 35; ES, exon skip; HNRNPA2B1, heterogeneous nuclear ribonucleoprotein A2/B1; INTS1, integrator complex subunit 1; lncRNA, long non-coding RNA; LUC7L2, LUC7 Like 2; MDS, myelodysplastic

[1] Zhongnan Hospital of Wuhan University, Wuhan, China
[2] Hubei Key Laboratory of Tumor Biological Behaviors, Wuhan, China
[3] Hubei Cancer Clinical Study Center, Wuhan, China
[4] Cancer Science Institute of Singapore, National University of Singapore, Singapore, Singapore

Corresponding Authors:
Hong-Bing Cai, MD, Department of Gynecological Oncology, Zhongnan Hospital of Wuhan University, 169 Donghu Road, Wuhan City, China.
Email: chb21051@163.com

Mengyuan Dai, MD, Department of Gynecological Oncology, Zhongnan Hospital of Wuhan University, 169 Donghu Rd., Wuhan City, China.
Email: mengyuandai@whu.edu.cn

syndrome; ME, mutually exclusive exon; MFSD11, major facilitator superfamily domain containing 11; mRNA, messenger RNA; OS, overall survival; OV, ovarian cancer; PSI, percent spliced-in; RI, retained intron; SF, splicing factor; STIC, serous intraepithelial carcinoma; SYNCRIP, synaptotagmin binding cytoplasmic RNA interacting protein; TCGA, The Cancer Genome Atlas.

Received: August 2, 2021; Revised: November 15, 2021; Accepted: November 29, 2021.

Introduction

Ovarian cancer (OV) is the most lethal malignancy of gynecological malignant tumors and is still one of the leading causes of cancer-related deaths in women worldwide. Up to 70% of patient deaths are due to the advanced stage. At present, the standard treatment for OV is surgery followed by a combination of chemotherapy.[1] However, 70% of OV patients eventually developed resistance to chemotherapy and recurrence with severe distant metastasis.[2] This suggests that the poor prognosis of OV is still a challenge that needs to be solved urgently. Some scholars have proposed, global splicing inhibition using small molecules blocking the spliceosome or SF-modifying enzymes to block the proliferation of cancer cells.[3] To improve the prognosis of OV and increase the survival rate of OV patients, we urgently need a robust method that can predict the prognosis of patients with OV in advance.

Alternative splicing (AS) widely exists in eukaryotic cells and plays an important role in the posttranscriptional regulation mechanism, which can regulate gene expression and increase protein diversity,[4] in normal physiological processes, some researchers have confirmed that most human genes have undergone the regulation of AS,[5] and regulate the binding between the protein and other cell components, such as nucleic acid and cell membrane.[6] Abnormal AS mutations affect the protein domain family and promote the occurrence, development, and invasion of tumors by disrupting protein interactions in cancer-related pathways.[7] More and more evidence has shown that abnormal AS is the basis of cancer.[3] However, the role of AS in OV remains unclear.

A splicing factor (SF) is a regulatory element of AS and plays an important role in the occurrence and development of tumors.[8] RNA sequencing revealed the changes of relevant AS events caused by SFs mutations.[9] SFs and AS events jointly establish a monitoring system network, and the coordinated SFs–AS network can regulate the growth and development of tissues and organs. And the dysregulation network is associated with the occurrence and development of cancer,[10] incorrectly expressed SFs may lead to abnormal mutations of AS in cancer, which in turn produces specific protein subtypes.[11]

Although many studies have suggested that abnormal AS events play an important role in the occurrence and development of OV,[12] there is still a lack of analysis of the complete survival status and systemic regulatory network of OV. We collected data from The Cancer Genome Atlas (TCGA) database for OV to assess the correlation between AS events and overall survival (OS) of OV, established a stable prognostic model, and performed network analysis on SFs–AS. We also attempted to construct prognostic nomograms of OV based on AS events. The findings of this study will help reveal the underlying mechanism of OV and provide a basis for improving the prognosis of OV patients.

Materials and Methods

Collect AS Events From the TCGA Database

The RNA-seq data and clinical information of OV patients were collected from the TCGA database (https://cancergenome.nih.gov/). Information of 7 types of AS events was collected from the TCGA SpliceSeq database (https://bioinformatics.mdanderson.org/TCGASpliceSeq/).[13] The percent spliced-in (PSI) value defines the profile of AS events, and the range of PSI is 0 to 1. To generate a set of AS events that are as reliable as possible, we implemented strict filtering conditions, that is, to filter out samples with a PSI value >75. Each AS event was represented by a combination of gene symbol, splicing type, and splicing ID number. We only included patients who survived more than 90 days and excluded patients whose death were not due to the tumor itself but other factors (such as surgical complications), finally, 384 patients were included in our study cohort.

Identify Survival-Related AS Events

For various types of AS events, OV patients were divided into 2 groups according to the median of the PSI value. Univariate Cox regression analysis was used to detect 7 types of survival-related AS events, and then an upset chart was drawn. Finally, the top 20 most significant AS events among the 7 types of AS events were displayed in the form of bubble charts.

Use AS Events to Build Predictive Models for OV Patients

To avoid overfitting the model, we performed the least absolute shrinkage and selection operator (LASSO) regression.[14] Then, to determine the penalty parameter lambda, we used the "glmnet" package for cross-validation. To determine the potential survival-related AS events, the optimal lambda value corresponding to the minimum value of the average cross-validation error was determined. Finally, the prediction model was generated based on multiple Cox regression analyses.

Then the risk score of each predictive model was calculated based on the sum of the product of the PSI value of the identified AS events and the corresponding coefficient generated from the Cox model. According to the median risk assessment, OV patients were divided into high-risk and low-risk groups.

The Kaplan–Meier survival analysis on the 7 AS events prediction models and the final prediction model were performed. Then we drew the receiver operating characteristic (ROC) curve for 1, 3, and 5 years, and used the area under the curve (AUC) value to determine the accuracy of each prediction model.

Establishment of Clinical Nomogram

To more effectively predict the individual survival probability and prognosis of OV, we performed univariate and multivariate Cox regression analysis on the collected clinical information and risk scores of OV patients and generated a predictive nomogram for the prognosis of patients with OV. Then we used the calibration curves to test the consistency between the predicted results and the actual results and evaluated the value of the nomogram in predicting the prognosis of OV.

Construction of SFs–AS Regulation Network

We obtained the SFs from the SpliceAid2 database (http://www.introni.it/splicing.html). Univariate Cox regression analysis was performed to search OS-related SFs, and Kaplan–Meier survival analysis was used for deeper verification. To explore the relationship between the PSI value of AS events and the expression of SFs that correlate with OS, Spearman correlation analysis was used, and a network was established using Cytoscape (version 3.5.1). Finally, the Human Protein Atlas database was used to validate the protein expression level of SFs with high correlation.

Statistical Analysis

All statistical analysis uses R software 3.5.0, P-value <0.05 is considered statistically significant.

Results

Overview of AS Events in the TCGA–OV Cohort

AS events can be divided into the following 7 types, including Exon Skip (ES), Alternate Promoter (AP), Alternate Terminator (AT), Alternate Donor site (AD), Alternate Acceptor site (AA), Mutually Exclusive exons (ME), and Retained Intron (RI). We obtained basic information of AS events in 384 OV patients from the TCGA SpliceSeq database. A total of 48,049 AS events were detected from 10,582 genes, of which 4006 AAs were detected from 2777 genes, and 3497 ADs were detected from 2389 genes, 9689 APs were detected from 3901 genes, 8453 ATs were detected from 3691 genes, 19,251 ESs were detected from 6931 genes, 207 MEs were detected from 201 genes, 2946 RIs were detected from 1951 genes (Table 1). Among them, ESs accounted for about 40%, which suggested that ES was the main type of AS event in OV patients. In addition, AS events in OV samples showed that a single gene had multiple types of AS events (Figure 1A).

Table 1. Overview of Total AS Events and OS-Related AS Events.

	Total AS events		OS-related AS events	
Type	AS events	Genes	AS events	Genes
AA	4006	2777	119	115
AD	3497	2389	117	115
AP	9689	3901	275	196
AT	8453	3691	201	136
ES	19251	6931	711	586
ME	207	201	8	8
RI	2946	1951	92	89
All	48049	10582	1523	1171

Abbreviations: AA, acceptor site; AD, alternate donor site; AP, alternate promoter; AS, alternative splicing; AT, alternate terminator; ES, exon skip; OS, overall survival; RI, retained intron; ME, mutually exclusive exon.

The OS-Related AS Events of OV

To screen out AS events related to OS in OV, we used univariate Cox analysis, the results showed that there were 1523 AS events in 1171 genes related to OS, of which 119 AA events in 115 genes, 117 AD events in 115 genes, 275 AP events in 196 genes, and 201 AT events in 136 genes, 711 ES events in 586 genes, 8 ME events in 8 genes, and 92 RI events in 89 genes (Table 1). A volcano plot was provided to show the AS events related to OS (Figure 1C). It can be seen from the UpSet plot that a single gene may have up to 7 types of AS events related to OS (Figure 1B).

In addition, we used bubble plots to show the top 20 most significant OS-related AS events (if available) (Figure 2). It is not difficult to see from the results that a large part of AS events in RI, ES, AA, and AD were prognostic factors with a good tendency. In addition, a gene can handle AS events that have a clear opposite effect on survival, and if they are restricted to the transcriptome level, they cannot be detected.

Construct a Prognostic Prediction Model for OV Patients

For each type of AS events, the hazards ratios (HRs) of the most significant AS events (if available) were selected and constructed a predictive model based on the AS events. Then 16 AAs, 14 ADs, 13 APs, 11 ATs, 11 ESs, 7 MEs, and 9 RIs, all 7 AS events related to OS were selected (Table 2) and constructed a predictive model based on the AS events. We calculated the risk score based on the selected AS events, set the median risk score, and divided OV patients into 2 groups based on the risk score, patients below the median risk score were classified into the low-risk group and vice versa. We set up 7 predictive models based on the risk score curves and displayed the survival status distribution of low-risk and high-risk groups in the heat maps (Figure 3). To explore whether there were differences in the survival rate between the high-risk group and the low-risk group, Kaplan–Meier survival analyses were performed (Figure 4D–J), the results showed that the survival rate of OV patients in the high-risk groups was significantly lower

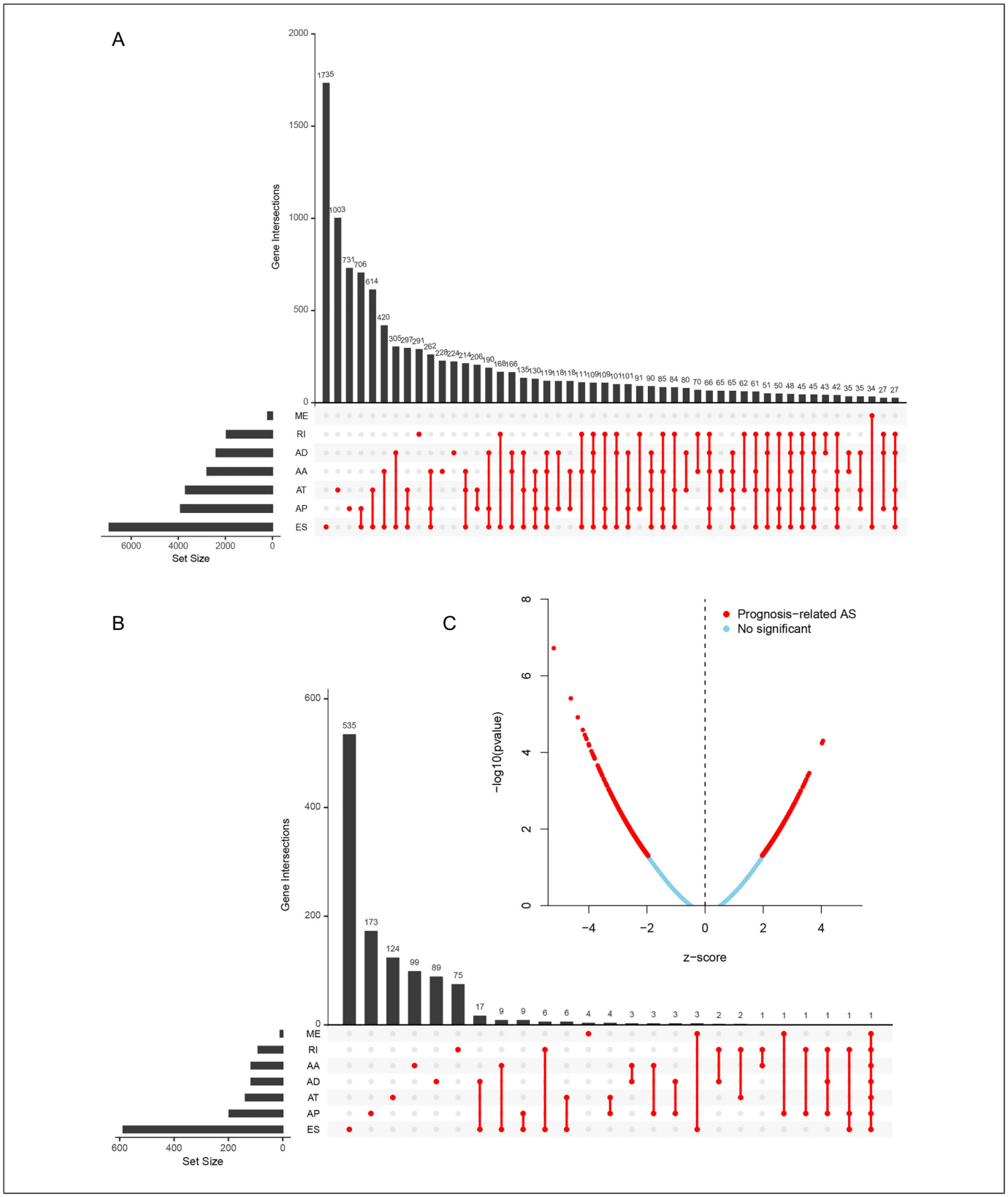

Figure 1. UpSet plot of AS events in OV. (A) The number of ES, AP, AT, AD, AA, ME, and RI in OV patients. (B) The number of 7 types of AS events related to prognosis in OV patients. (C) Volcano plot of AS events related to prognosis (red dots), no significant AS events (blue dots). Abbreviations: AS, alternative splicing; OV, ovarian cancer; ES, exon skip; AP, alternate promoter; AT, alternate terminator; AD, alternate donor site; AA, acceptor site; ME, mutually exclusive exon; RI, retained intron.

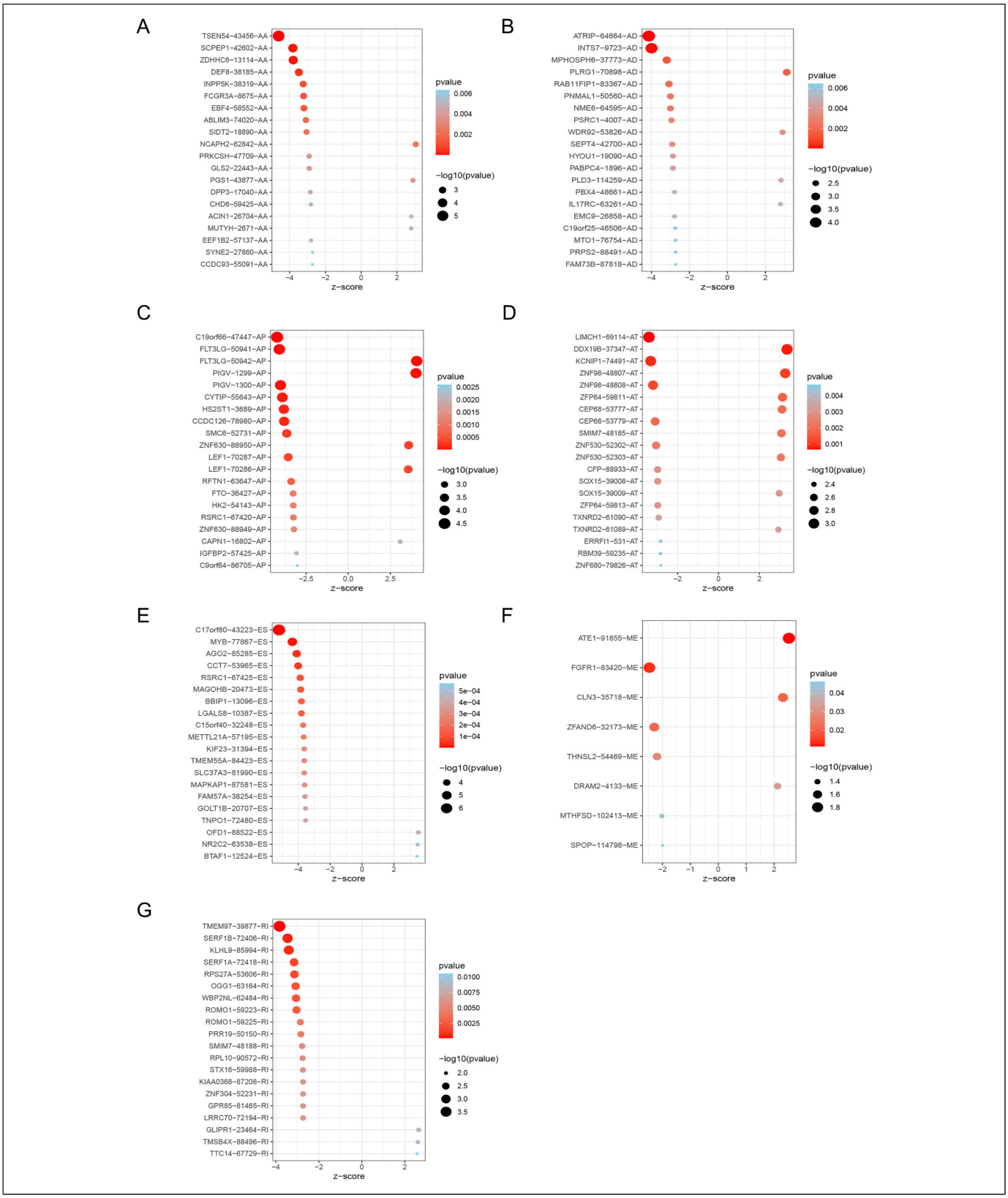

Figure 2. Bubble plots of 7 types of prognostic-related AS events. (A-F) The top 20 AS events with the highest prognostic correlation among AA, AD, AP, AT, ES, and RI. (G) Eight AS events related to prognosis in ME.

Abbreviations: AA, acceptor site; AD, alternate donor site; AP, alternate promoter; AT, alternate terminator; ES, exon skip; RI, retained intron; ME, mutually exclusive exon.

Table 2. Information of AS Events Used for Construction of Prediction Model

Type	Id	Coef	HR	HR.95L	HR.95H	*P*-value
AA	TSEN54|43456|AA	−34.65	8.99×10^{-16}	1.13×10^{-21}	7.18×10^{-10}	5.84×10^{-7}
	SCPEP1|42602|AA	−3.62	0.0267	0.0027	0.264	.001956801
	ZDHHC6|13114|AA	−5.97	0.00255	7.68×10^{-5}	0.085	.000841742
	DEF8|38185|AA	−10.8	2.03×10^{-5}	2.87×10^{-8}	0.0144	.001250737
	INPP5K|38319|AA	−3.14	0.0434	0.0053	0.356	.003488113
	FCGR3A|8675|AA	−2.56	0.077	0.0117	0.508	.007743499
	ABLIM3|74020|AA	−3.78	0.0228	0.000443	1.176	.060112605
	SIDT2|18890|AA	−5.28	0.00509	2.66×10^{-5}	0.976	.048940402
	NCAPH2|62842|AA	3.97	53.2	0.781	3623.09	.065000917
	PRKCSH|47709|AA	−5.11	0.00603	0.0005	0.0727	5.73×10^{-5}
	DPP3|17040|AA	−2.65	0.0704	0.00493	1	.050308256
	CHD6|59425|AA	−15.15	2.63×10^{-7}	2.21×10^{-11}	0.00312	.001551075
	ACIN1|26704|AA	5.55	256.9	7.67	8600.61	.001951511
	MUTYH|2671|AA	3.27	26.37	4.22	165	.000468794
	EEF1B2|57137|AA	−1.20	0.3	0.0878	1.028	.05541612
	CCDC93|55091|AA	−9.00	0.000124	1.49×10^{-6}	0.0103	6.57×10^{-5}
AD	ATRIP|64664|AD	−4.59	0.0101	0.000761	0.135	.000513397
	INTS7|9723|AD	−5.61	0.00367	0.000444	0.0303	1.89909×10^{-7}
	PLRG1|70898|AD	8.39	4418.17	0.396	49306417.57	.077546266
	PNMAL1|50560|AD	−3.21	0.0402	0.00916	0.177	2.10683×10^{-5}
	NME6|64595|AD	−1.46	0.232	0.0747	0.723	.011705224
	PSRC1|4007|AD	−1.91	0.148	0.0535	0.41	.000239824
	HYOU1|19090|AD	−1.33	0.264	0.053	1.315	.104073558
	PABPC4|1896|AD	−2.49	0.083	0.0133	0.516	.007622437
	PLD3|114259|AD	2.99	20.04	2.764	145.253	.003018019
	PBX4|48661|AD	−1.77	0.171	0.0502	0.58	.004611542
	IL17RC|63261|AD	2.62	13.73	3.985	47.305	3.31833×10^{-5}
	C19orf25|46506|AD	−1.79	0.167	0.0187	1.496	.109673555
	MTO1|76754|AD	−1.47	0.231	0.0385	1.382	.108260102
	FAM73B|87818|AD	−1.43	0.24	0.101	0.572	.001271861
AP	C19orf66|47447|AP	−5.23	0.00538	0.000679	0.0427	7.57797×10^{-7}
	FLT3LG|50941|AP	−1.88	0.153	0.0402	0.581	.005829405
	PIGV|1299|AP	1.4	4.05	1.531	10.714	.004827454
	CYTIP|55643|AP	−9.12	0.000109	4.196×10^{-7}	0.0286	.001316224
	HS2ST1|3689|AP	−12.84	2.67×10^{-6}	3.50×10^{-8}	0.00203	.000150034
	SMC6|52731|AP	−4.57	0.0103	0.0000793	1.345	.065649937
	ZNF630|88950|AP	2.33	10.269	1.7566	60.042	.009734321
	LEF1|70287|AP	−3.78	0.0227	0.000891	0.58	.022026696
	RFTN1|63647|AP	−12.57	3.46×10^{-6}	1.86×10^{-8}	0.00643	.001059918
	FTO|36427|AP	−10.01	0.0000448	3.31×10^{-8}	0.0606	.006493959
	HK2|54143|AP	−4.64	0.00968	0.000182	0.515	.022188718
	RSRC1|67420|AP	−4.33	0.0131	0.0013	0.132	.000236378
	CAPN1|16802|AP	1.44	4.224	0.586	30.43	.152643133
AT	LIMCH1|69114|AT	−13.48	1.40×10^{-6}	1.26×10^{-9}	0.00155	.000164089
	DDX19B|37347|AT	11.38	86718.22	40.94	183684420.7	.003614395
	KCNIP1|74491|AT	−5.08	0.00619	0.00032	0.12	.000776074
	ZNF98|48807|AT	0.83	2.301	1.171	4.52	.015618209
	ZFP64|59811|AT	3.66	39.027	2.749	554.046	.006788653
	CEP68|53777|AT	5.08	161.31	3.132	8308.248	.011483088
	SMIM7|48185|AT	2.01	7.437	1.466	37.727	.015444174
	ZNF530|52303|AT	1.03	2.813	1.183	6.691	.019294347
	CFP|88933|AT	−0.7	0.498	0.331	0.751	.000858486
	SOX15|39009|AT	0.96	2.619	1.204	5.699	.015219809
	ERRFI1|531|AT	−14.52	4.93×10^{-7}	4.58×10^{-11}	0.00529	.002164215
ES	C17orf80|43223|ES	−4.06	0.0172	0.00396	0.0746	5.77922×10^{-5}
	MYB|77867|ES	−33.85	1.98×10^{-15}	6.11×10^{-21}	6.44×10^{-10}	1.70709×10^{-5}
	AGO2|85285|ES	−9.58	0.0000688	4.98×10^{-7}	0.0095	.000137973
	CCT7|53965|ES	−2.44	0.087	0.0257	0.295	8.73533×10^{-5}

(continued)

Table 2. (continued)

Type	Id	Coef	HR	HR.95L	HR.95H	*P*-value
	TMEM55A|84423|ES	−4.31	0.0134	0.00157	0.115	8.26806×10^{-5}
	SLC37A3|81990|ES	−10.85	0.0000194	2.38×10^{-8}	0.0159	.00152398
	MAPKAP1|87581|ES	−17.10	3.74×10^{-8}	4.30×10^{-12}	0.000326	.000220058
	FAM57A|38254|ES	−3.52	0.0295	0.00436	0.199	.000302154
	OFD1|88522|ES	2.87	17.723	4.56	68.884	3.31806×10^{-5}
	NR2C2|63538|ES	2.08	7.991	2.684	23.791	.000188967
	BTAF1|12524|ES	1.53	4.605	0.934	22.701	.060635638
ME	ATE1|91855|ME	1.53	4.631	1.617	13.263	.004307715
	FGFR1|83420|ME	−12.21	5.00×10^{-6}	1.43×10^{-10}	0.175	.022215226
	CLN3|35718|ME	2.88	17.752	1.853	170.060	.01259676
	ZFAND6|32173|ME	−7.16	0.000776	0.0000114	0.0528	.00087917
	THNSL2|54469|ME	−1.63	0.195	0.0339	1.125	.067480213
	DRAM2|4133|ME	7.01	1109.5	0.559	2204018.37	.070352141
	MTHFSD|102413|ME	−1.70	0.182	0.0247	1.34	.094387682
RI	SERF1B|72406|RI	−9.98	0.0000464	8.21×10^{-9}	0.263	.023613219
	OGG1|63164|RI	−1.23	0.293	0.0855	1.003	.050639314
	WBP2NL|62484|RI	−0.92	0.398	0.139	1.136	.085125839
	ROMO1|59223|RI	−3.19	0.0413	0.00251	0.682	.025884513
	SMIM7|48188|RI	−5.72	0.00327	0.000026	0.411	.020311408
	RPL10|90572|RI	−0.69	0.499	0.208	1.199	.120351008
	STX16|59988|RI	−6.02	0.00243	0.00000555	1.065	.052404028
	TMSB4X|88496|RI	8.28	3936.173	13.841	1119408.398	.004086336
	TTC14|67729|RI	1.53	4.627	0.948	22.599	.058314362
All	C17orf80|43223|ES	−3.17	0.0419	0.00629	0.28	.001055862
	TSEN54|43456|AA	−29.68	1.29×10^{-13}	1.43×10^{-20}	0.00000116	.000280645
	MYB|77867|ES	−23.87	4.31×10^{-11}	4.76×10^{-17}	0.000039	.000648182
	C19orf66|47447|AP	−2.78	0.0619	0.00462	0.829	.035556265
	ATRIP|64664|AD	−5.39	0.00456	0.000357	0.0582	.0000336
	AGO2|85285|ES	−11.32	0.0000122	0.00000007	0.00211	.000017
	FLT3LG|50941|AP	−2.09	0.123	0.0323	0.469	.0021431
	PIGV|1299|AP	1.28	3.582	1.415	9.067	.007097646
	CCT7|53965|ES	−2.64	0.071	0.0187	0.27	.000104182
	CYTIP|55643|AP	−10.89	0.0000186	1.07×10^{-7}	0.00321	.0000343
	RSRC1|67425|ES	-4.36	0.0128	0.00133	0.124	.000163931
	ZDHHC6|13114|AA	-5.72	0.00326	0.000121	0.0878	.000654625

Abbreviations: AA, acceptor site; AD, alternate donor site; AP, alternate promoter; AS, alternative splicing; AT, alternate terminator; ES, exon skip; HR, hazard ratio; RI, retained intron; ME, mutually exclusive exon.

than that in the low-risk groups. It showed that the 7 prediction models could effectively predict the prognosis of low-risk and high-risk OV patients. According to the results of ROC curves of every single type of AS event in 1, 3, and 5 years, it turned out that these 7 prognostic models had great predictive efficiency (Figure 4A-C).

To construct the final predictive model, 12 AS events related to OS were finally selected using LASSO regression (Figure 5A and B). The risk score curve of the final prediction model, the distribution of survival status of high-risk and low-risk groups, and the heat map of the PSI value of AS events were showed (Figure 5D–F). We used the Kaplan–Meier survival analysis to detect the prediction results of the model, the final prediction model could effectively distinguish the prognosis results of OV patients between low-risk and high-risk groups (Figure 5C). According to the results of the ROC curves, the final prediction model showed strong prediction efficiency, with the maximum AUC in 1, 3, and 5 years being 0.785, 0.681, and 0.781, respectively (Figure 5G-I).

Construction of AS-Clinicopathologic Nomogram

We evaluated the risk score (all), age, and grade using univariate and multivariate Cox regression analysis to determine the prognostic value of OV. The results of univariate Cox regression analysis ($P<0.001$) and multiple Cox regression analysis ($P<0.001$) (Figure 6A and B) indicated that the risk score (all) was an independent risk factor for predicting the prognosis of OV patients. The nomogram was constructed on the basis of risk score (all), age, and grade using multivariate Cox regression analysis to predict survival and prognosis of OV patients at 1, 3, and 5 years directly (Figure 6C). The results of the calibration curve (Figure 6D-F)

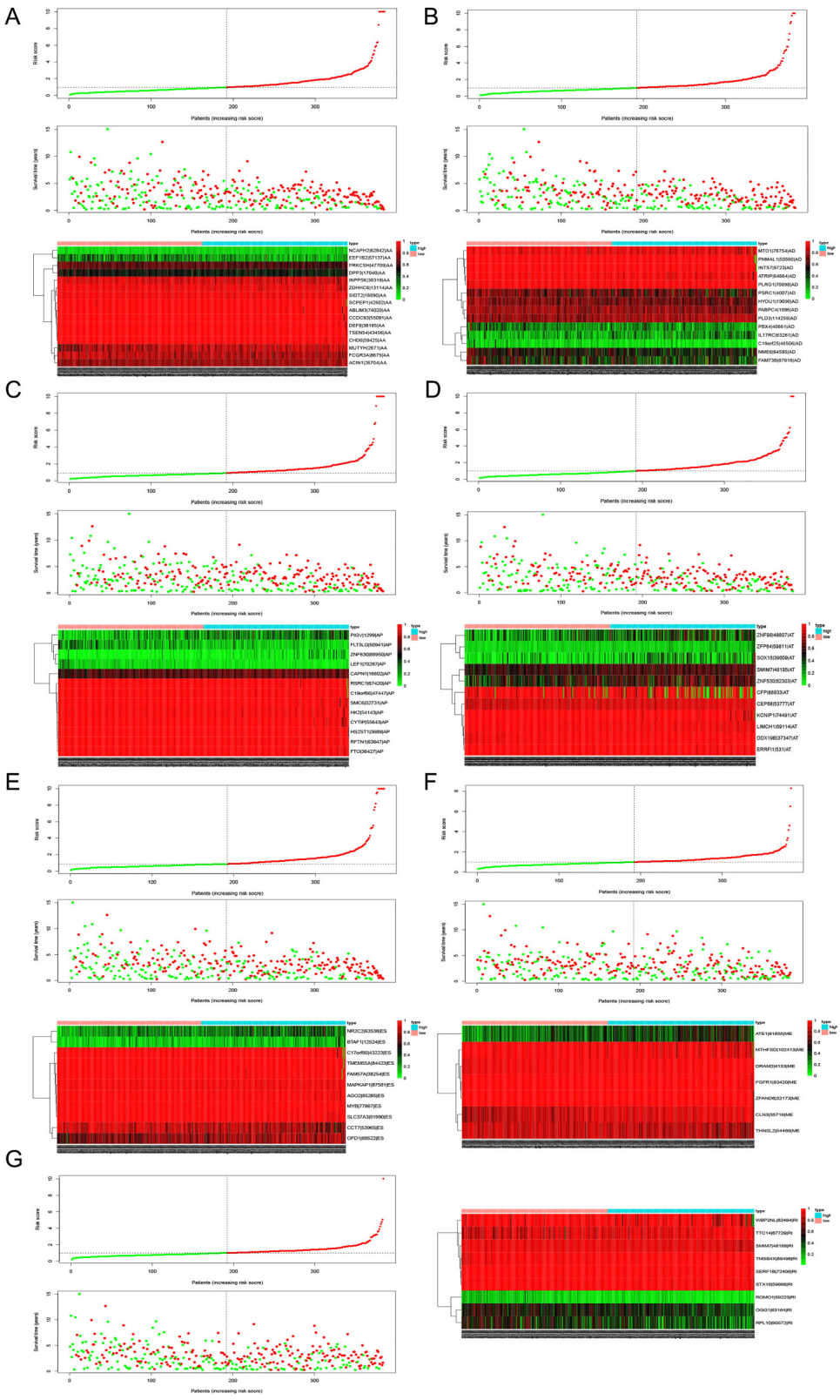

Figure 3. Analysis of a predictive model of OV patients. (A-G) Set the median risk score. OV patients below the median risk score belong to the low-risk group, and OV patients above the median risk score belong to the high-risk group. The upper part of each set shows the risk score curve of 7 types of AS events, the middle part shows the survival status of OV patients, and the bottom part shows the calorie map of 7 types of AS events.

Abbreviations: OV, ovarian cancer; AS, alternative splicing.

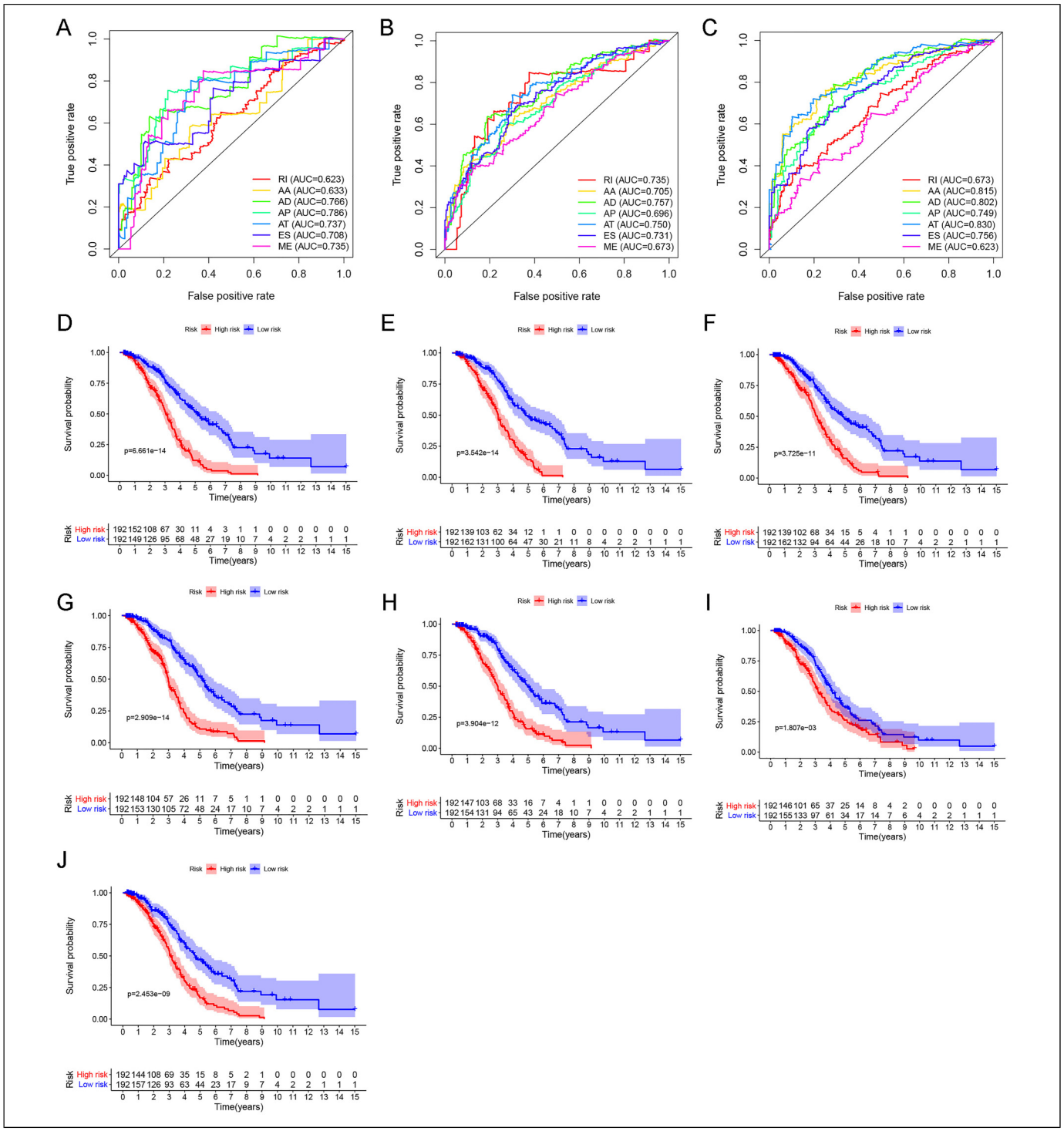

Figure 4. The ROC prediction model curve and Kaplan–Meier prediction model for OV patients. (A-C) The prediction models were constructed by 7 types of AS events for 1, 3, and 5 years ROC curves. (D-J) Seven types of AS event prediction models Kaplan–Meier curve.
Abbreviations: OV, ovarian cancer; AS, alternative splicing; ROC, receiver operating characteristic.

showed that 1, 3, and 5 years prediction results of the constructed nomogram were in good agreement with the actual observation. It indicated that the nomogram was of great significance for the survival and prognosis prediction of OV patients.

The Regulation Network of SFs and Prognostic-Related AS Events

SF is a protein factor involved in the splicing process of RNA precursors. Abnormal expression of SFs can lead to the

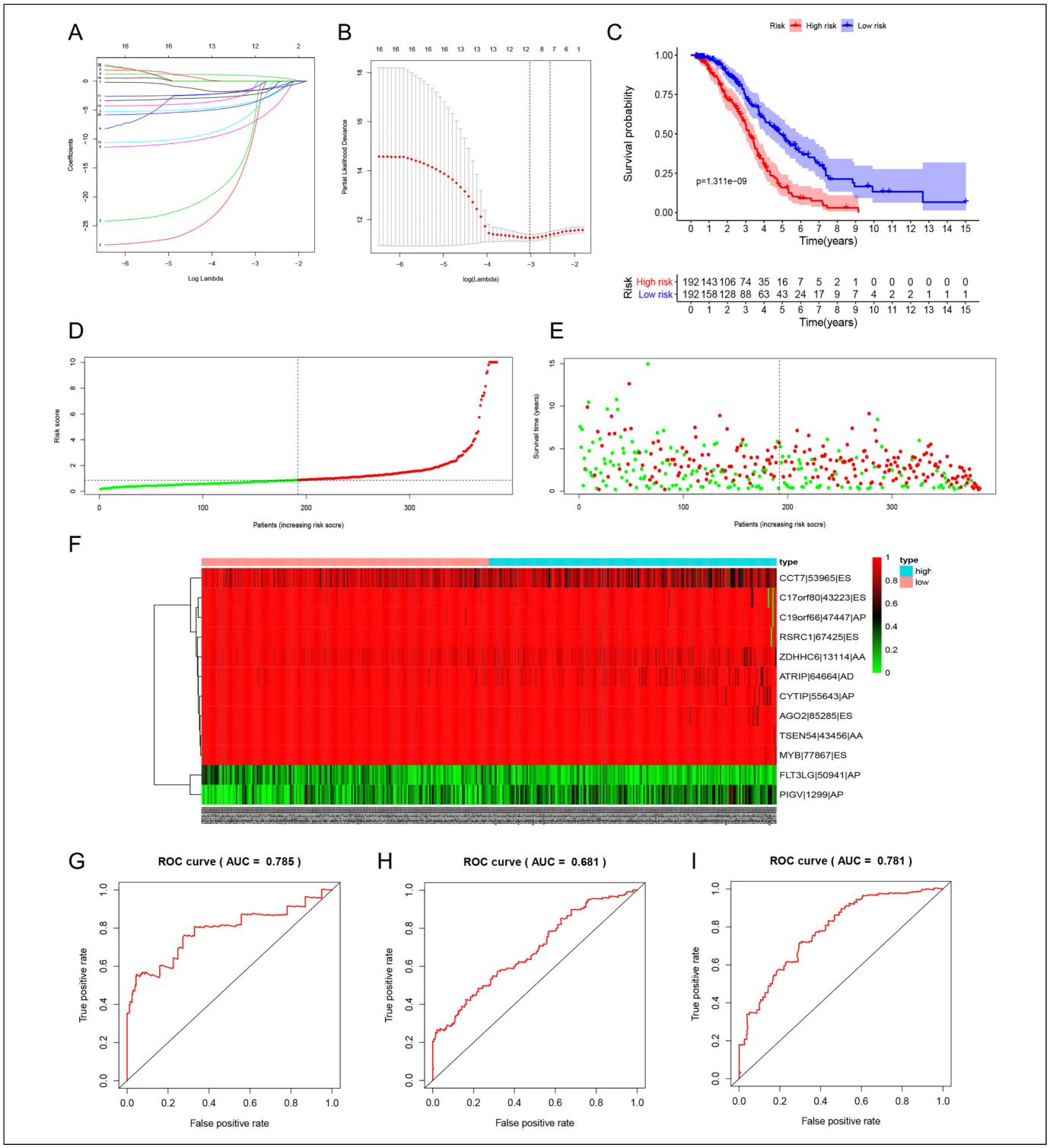

Figure 5. Establishment and assessment of the final prediction model. (A) The LASSO regression coefficient of AS events correlated with OS. (B) Select the best parameter in the model, and mark the vertical dashed line at the best value. (C) Kaplan–Meier curve of the final prediction model. (D) The final prediction model risk score curve. (E) Survival status of OV patients. (F) Final prediction model AS event heating value map. (G-I) One, 3, and 5 years ROC curve of the final prediction model.

Abbreviations: LASSO, least absolute shrinkage and selection operator; AS, alternate splicing; OS, overall survival; OV, ovarian cancer; ROC, receiver operating characteristic.

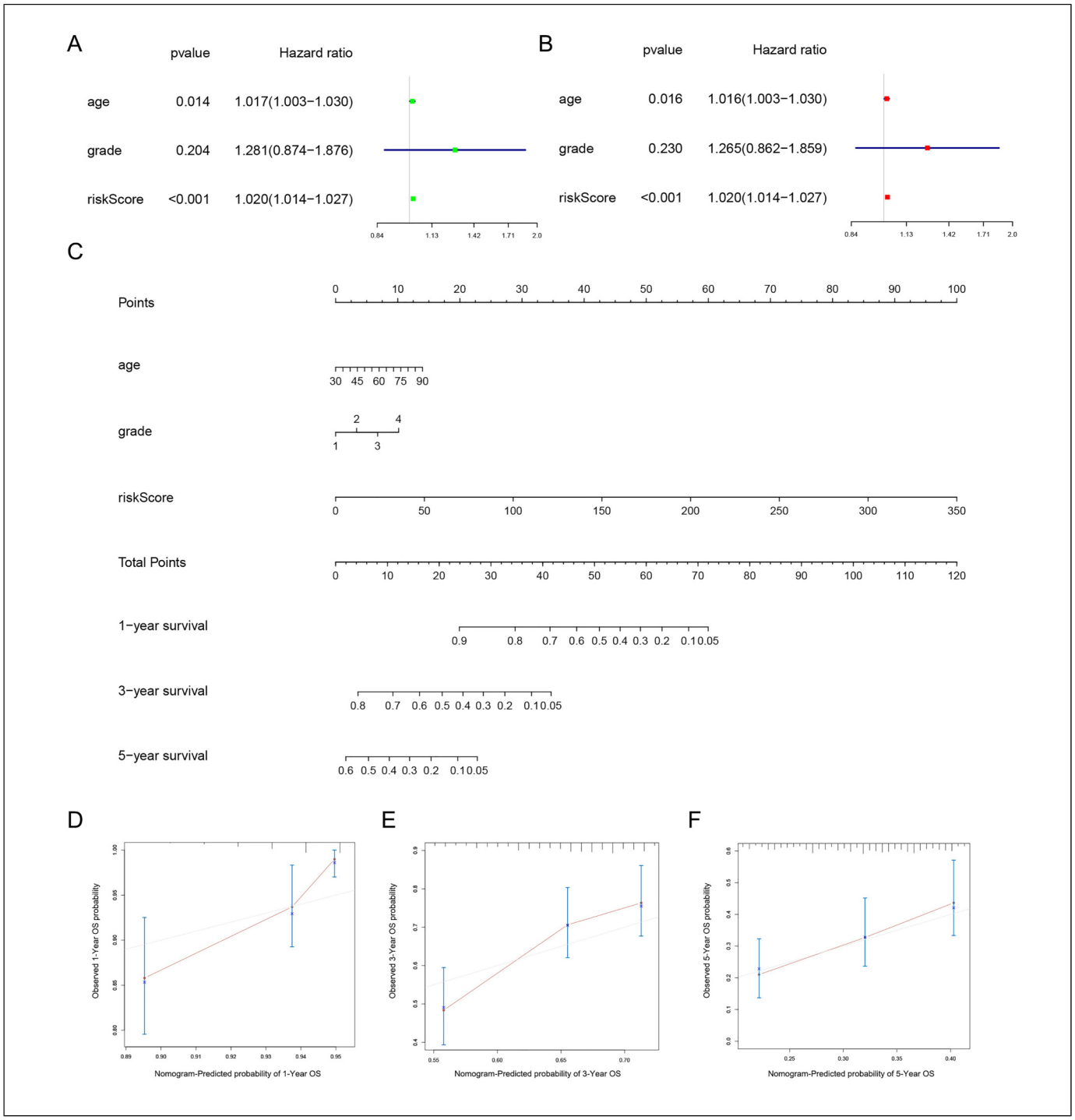

Figure 6. A clinicopathological nomogram can predict the survival rate of OV patients. (A) Univariate Cox regression analysis of risk score (all), age, and grade. (B) Multivariate Cox regression analysis of risk score (all), age, and grade. (C) Incorporate the age, grade, and risk score of OV patients to establish a prognostic nomogram, predict the 1, 3, and 5 years survival rates of OV patients. (D-F) Calibration plot of the AS-clinicopathologic nomogram.
Abbreviations: OV, ovarian cancer; AS, alternate splicing.

change of AS of genes and the formation of specific cancer-promoting splicing isomers, thus leading to the occurrence of cancer. We collected 71 SFs from the SpliceAid2 database (http://www.introni.it/splicing.html) to explore the relation between the survival interaction of genes and SFs. A total of 24 prognostic-related SFs of OV patients were obtained using univariate Cox analysis (Figure 7A). To narrow the scope, 10 candidate SFs were obtained using Kaplan–Meier survival

analysis (Supplemental Figure 1). To explore the degree of correlation between OS-related AS events and SFs, a spearman correlation analysis was carried out and 8 SFs were obtained which were most significantly related to AS events, including major facilitator superfamily domain containing 11 (MFSD11), synaptotagmin binding cytoplasmic RNA interacting protein (SYNCRIP), DEAH-box helicase 35 (DHX35), CWC15, integrator complex subunit 1 (INTS1), LUC7 Like 2 (LUC7L2), cell cycle and apoptosis regulator 1 (CCAR1), and heterogeneous nuclear ribonucleoprotein A2/B1 (HNRNPA2B1). The regulatory network consisted of 58 AS events that were highly relevant to OS, of which 30 AS events were favorable (red dots), and 28 AS events were unfavorable (green dots) (Figure 7B). Finally, these SFs were verified the protein level using The Human Protein Atlas databases (Supplemental Figure 2).

Discussion

OV is a gynecological malignant tumor with a high incidence and high mortality rate,[2] and the 5-year survival did not exceed 45%.[15] OV can develop from ovarian superficial epithelium or serous tubal intraepithelial carcinoma (STIC), and it is usually diagnosed at an advanced stage,[16] accompanied by symptoms such as extensive abdominal metastasis, abdominal masses, massive abdominal effusion, weight loss, and anemia. However, the mechanism of its occurrence and metastasis is not very clear, the early diagnosis of OV and the discovery of biomarkers for predicting survival are very important.[17] With the development of various gene sequencing technologies, many potential prognostic and survival markers of OV have been discovered, such as microRNA,[18] circRNA,[19] long noncoding RNA (lncRNA),[20,21] however, these studies were limited to the transcription level, and there were few studies on the posttranscriptional mechanism of the occurrence and development of OV. In recent years, significant progress has been made in the research on the role of AS events in the occurrence and development of malignant tumors, but a systematic analysis of AS events in OV is still lacking, which means that AS events have great potential in the research of OV.

AS is the RNA exons produced by the transcription of genes or messenger RNA (mRNA) precursors that are reconnected by RNA shearing in a variety of ways, which can translate mRNA into different protein isoforms, thereby increasing protein diversity.[22] More and more evidence has shown that abnormal AS plays a key role in the various processes of tumorigenesis.[23] For example, the regulatory kinase cyclin-dependent kinase 12 (CDK12) has an evolutionary conservation effect, but CDK12 regulates selective mRNA splicing and activates DNA damage response activators ATM and DNAJB6 in OV, affecting cell invasion and promoting tumorigenesis.[24] Proto-oncogene (RON) is overexpressed in OV and has a specifically expressed AS subtype.[25] These indicate that AS is of great significance in the study of abnormal gene regulation to promote the occurrence and development of OV.

In this study, we detected 48,049 AS events from 10,528 genes, suggesting that AS is a common procedure in OV, ES was the main component of AS events, and 1523 AS events were detected in 1171 genes related to OS. LASSO regression was used to select the AS events with the highest correlation with OS to construct the prediction model, in addition, to construct prediction models for single AS events, we integrated 7 AS events to construct a final prediction model. The prediction efficiency of the prediction model was significant (AUC = 0.785). PSI values were used to directly quantify the shear change ratios of 7 AS events. In addition, combining AS events with corresponding clinical parameters, risk score, age, and grade were integrated to construct a nomogram, and constructed a clinical prediction nomogram to directly evaluate the survival prognosis of an individual in 1, 3, and 5 years. The calibration curve showed that the predicted results of the model were consistent with the actual observations. This means that the use of clinical nomograms will be a benefit to clinical work.

The precise regulation of AS is achieved by the combination of SFs and splicing elements of specific genes, thereby affecting the selection of exons and splicing sites,[26] abnormal expression of SFs is likely to lead to differential expression of selective shear processes,[27] we performed Spearman correlation analysis on the obtained SFs, and finally obtained 8 SFs that were most significantly related to survival, including CCAR1, LUC7L2, SYNCRIP, HNRNPA2B1, DHX35, CWC15, INTS1, and MFSD11, and constructed the AS–SFs analysis network based on these 8 SFs. CCAR1 is one of the components of the Wnt/β-catenin signal transduction pathway, increased expression of CCAR1 is related to the occurrence of gastric cancer.[28] CCAR1 can also bind to constitutive androstane receptor (CAR) to enhance CAR-inducing activity, thereby mediating the growth, migration, and invasion of liver cancer[29] and prostate cancer.[30] LUC7L2 is located on chromosome 7 and is mainly involved in myelodysplastic syndrome (MDS), LUC7L2[31,32] can be used as a target site for MDS screening and treatment,[33] and it is a highly conserved RNA binding protein whose amino-terminal binds to mRNA,[34] which regulates the microenvironment.[35] SYNCRIP is a differential gene between normal leukemia and myeloid leukemia, its deletion can increase the degree of apoptosis and differentiation, and delay the occurrence of leukemia.[36] HNRNPA2B1 is involved in coding neurodegeneration-related RNA binding protein,[37] and its ubiquitination is involved in the differential expression of lncRNA in liver cancer cells, after being inhibited, it can reduce the invasion and metastasis of liver cancer.[38] The study found that the occurrence of DHX35 variant ductal carcinoma of the pancreas is closely related.[39] Similarly, abnormal mutations in CWC15[40] and INTS1[41] cause changes in the splicing process, leading to abnormal posttranscriptional regulation and tumor occurrence. Currently, MFSD11 mutations have not been found to be related to tumorigenesis.

AS is a highly controlled process that relies on *cis*-regulatory elements and trans-regulatory factors.[42] Vivo experiments have

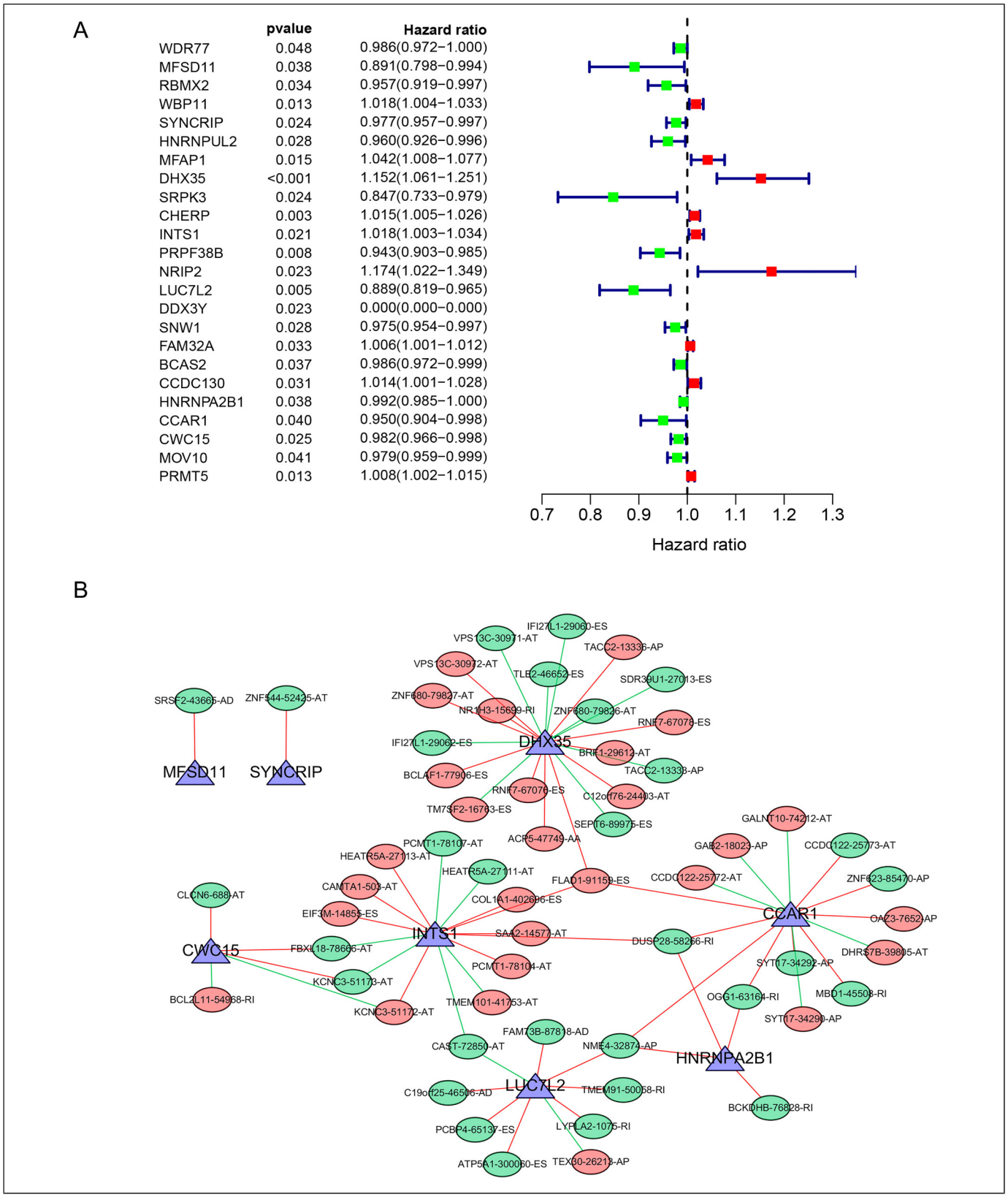

Figure 7. Correlation network regulated by SFs and OS-related AS events in OV. (A) Forest graph of AS events related to OS. Obtain 71 SFs from the database, and use univariate Cox regression analysis to obtain 24 OS-related SFs. (B) Regulation network of SFs and OS-related AS events. Green dots indicate OS-related SFs, red dots indicate favorable AS events, and green dots indicate unfavorable AS events. The red lines indicate a positive correlation and the green lines indicate a negative correlation.

Abbreviations: SF, splicing factor; OS, overall survival; AS, alternate splicing; OV, ovarian cancer.

confirmed that the regulation of specific AS site targets can effectively inhibit the occurrence of tumors.[43] In OV, AS plays an important role in reversing platinum resistance.[44] Therefore, we believe that using AS sites as potential targets for the treatment of OV can effectively improve the survival rate of OV patients.

Although our research shows the role of abnormal variants of AS events in OV, it still has certain limitations. First of all, our research data came from a public database with a small sample size. Second, this is a bioinformatics study that has not been verified by external functional tests. Due to the limitations of public data, the clinical data we obtained are incomplete, which makes us deviate from the actual results when constructing clinical prediction models. In short, we conducted a systematic analysis of OV on the basis of AS events, constructed a prognostic survival model for OV patients, and used the nomogram to predict the prognosis of individual patients. We also established an AS–SFs network to reveal SFs play a key role in the shear network. This is of great significance for the prognosis of OV and drug target treatment.

Acknowledgements

We would like to express our sincere thanks to Dr. Zhen Li for her excellent technical support and the public resources of TCGA databases.

Availability of Data and Materials

The data that support the findings of this study are openly available in the TCGA database at https://genomecancer.ucsc.edu/.

Funding

The authors disclosed receipt of the following financial support for the research, authorship, and/or publication of this article: This work was supported by the National Natural Science Foundation of China (81972447), National Natural Science Foundation of China Youth Project (82002770), Excellent Doctor (Post) Project of Zhongnan Hospital of Wuhan University (2020009), Fundamental Research Funds for the Central Universities (2042021kf0150). The funders had no role in study design, data collection, and analysis, decision to publish, or preparation of the manuscript.

Declaration of Conflicting Interests

The authors declared no potential conflicts of interest with respect to the research, authorship, and/or publication of this article.

ORCID iDs

Shijie Yao https://orcid.org/0000-0003-4648-5464
Yuwen Qi https://orcid.org/0000-0002-2420-2235

Supplemental Material

Supplemental material for this article is available online.

References

1. Odunsi K. Immunotherapy in ovarian cancer. *Ann Oncol*. 2017;28(suppl_8):viii1–viii7. doi:10.1093/annonc/mdx444
2. Grunewald T, Ledermann JA. Targeted therapies for ovarian cancer. *Best Pract Res Clin Obstet Gynaecol*. 2017;41:139–152. doi:10.1016/j.bpobgyn.2016.12.001
3. Urbanski LM, Leclair N, Anczukow O. Alternative-splicing defects in cancer: splicing regulators and their downstream targets, guiding the way to novel cancer therapeutics. *Wiley Interdiscip Rev RNA*. 2018;9(4):e1476. doi:10.1002/wrna.1476
4. Baralle FE, Giudice J. Alternative splicing as a regulator of development and tissue identity. *Nat Rev Mol Cell Biol*. 2017;18-(7):437–451. doi:10.1038/nrm.2017.27
5. Nilsen TW, Graveley BR. Expansion of the eukaryotic proteome by alternative splicing. *Nature*. 2010;463(7280):457–463. doi:10.1038/nature08909
6. Kelemen O, Convertini P, Zhang Z, et al. Function of alternative splicing. *Gene*. 2013;514(1):1–30. doi:10.1016/j.gene.2012.07.083
7. Climente-Gonzalez H, Porta-Pardo E, Godzik A, Eyras E. The functional impact of alternative splicing in cancer. *Cell Rep*. 2017;20(9):2215–2226. doi:10.1016/j.celrep.2017.08.012
8. Anczukow O, Krainer AR. Splicing-factor alterations in cancers. *RNA*. 2016;22(9):1285–1301. doi:10.1261/rna.057919.116
9. Seiler M, Peng S, Agrawal AA, et al. Somatic mutational landscape of splicing factor genes and their functional consequences across 33 cancer types. *Cell Rep*. 2018;23(1):282–296 e4. doi:10.1016/j.celrep.2018.01.088
10. Yoshida K, Ogawa S. Splicing factor mutations and cancer. *Wiley Interdiscip Rev RNA*. 2014;5(4):445–459. doi:10.1002/wrna.1222
11. Han H, Braunschweig U, Gonatopoulos-Pournatzis T, et al. Multilayered control of alternative splicing regulatory networks by transcription factors. *Mol Cell*. 2017;65(3):539–553 e7. doi:10.1016/j.molcel.2017.01.011
12. Zhu J, Chen Z, Yong L. Systematic profiling of alternative splicing signature reveals prognostic predictor for ovarian cancer. *Gynecol Oncol*. 2018;148(2):368–374. doi:10.1016/j.ygyno.2017.11.028
13. Ryan MC, Cleland J, Kim R, Wong WC, Weinstein JN. Spliceseq: a resource for analysis and visualization of RNA-Seq data on alternative splicing and its functional impacts. *Bioinformatics*. 2012;28(18):2385–2387. doi:10.1093/bioinformatics/bts452
14. Sauerbrei W, Royston P, Binder H. Selection of important variables and determination of functional form for continuous predictors in multivariable model building. *Stat Med*. 2007;26(30):5512–5528. doi:10.1002/sim.3148
15. Webb PM, Jordan SJ. Epidemiology of epithelial ovarian cancer. *Best Pract Res Clin Obstet Gynaecol*. 2017;41:3–14. doi:10.1016/j.bpobgyn.2016.08.006
16. Ottevanger PB. Ovarian cancer stem cells more questions than answers. *Semin Cancer Biol*. 2017;44:67–71. doi:10.1016/j.semcancer.2017.04.009
17. Muinao T, Deka Boruah HP, Pal M. Diagnostic and prognostic biomarkers in ovarian cancer and the potential roles of cancer stem cells—an updated review. *Exp Cell Res*. 2018;362(1):1–10. doi:10.1016/j.yexcr.2017.10.018
18. Deb B, Uddin A, Chakraborty S. miRNAs and ovarian cancer: an overview. *J Cell Physiol*. 2018;233(5):3846–3854. doi:10.1002/jcp.26095

19. Ning L, Long B, Zhang W, et al. Circular RNA profiling reveals circEXOC6B and circN4BP2L2 as novel prognostic biomarkers in epithelial ovarian cancer. *Int J Oncol*. 2018;53(6):2637–2646. doi:10.3892/ijo.2018.4566
20. Wang Y, Ren F, Chen P, Liu S, Song Z, Ma X. Effects of cytoreductive surgery plus hyperthermic intraperitoneal chemotherapy (HIPEC) versus cytoreductive surgery for ovarian cancer patients: a systematic review and meta-analysis. *Eur J Surg Oncol*. 2019;45(3):301–309. doi:10.1016/j.ejso.2018.10.528
21. Du W, Feng Z, Sun Q. LncRNA LINC00319 accelerates ovarian cancer progression through miR-423-5p/NACC1 pathway. *Biochem Biophys Res Commun*. 2018;507(1–4):198–202. doi:10.1016/j.bbrc.2018.11.006
22. Tress ML, Abascal F, Valencia A. Alternative splicing may not be the key to proteome complexity. *Trends Biochem Sci*. 2017;42(2):98–110. doi:10.1016/j.tibs.2016.08.008
23. David CJ, Manley JL. Alternative pre-mRNA splicing regulation in cancer: pathways and programs unhinged. *Genes Dev*. 2010;24-(21):2343–2364. doi:10.1101/gad.1973010
24. Tien JF, Mazloomian A, Cheng SG, et al. CDK12 regulates alternative last exon mRNA splicing and promotes breast cancer cell invasion. *Nucleic Acids Res*. 2017;45(11):6698–6716. doi:10.1093/nar/gkx187
25. Mayer S, Hirschfeld M, Jaeger M, et al. RON Alternative splicing regulation in primary ovarian cancer. *Oncol Rep*. 2015;34(1):423–430. doi:10.3892/or.2015.3995
26. Jyotsana N, Heuser M. Exploiting differential RNA splicing patterns: a potential new group of therapeutic targets in cancer. *Expert Opin Ther Targets*. 2018;22(2):107–121. doi:10.1080/14728222.2018.1417390
27. Klinck R, Bramard A, Inkel L, et al. Multiple alternative splicing markers for ovarian cancer. *Cancer Res*. 2008;68(3):657–663. doi:10.1158/0008-5472.CAN-07-2580
28. Chang TS, Wei KL, Lu CK, et al. Inhibition of CCAR1, a coactivator of beta-catenin, suppresses the proliferation and migration of gastric cancer cells. *Int J Mol Sci*. 2017;18(2):1–14. doi:10.3390/ijms18020460
29. Kanno Y, Zhao S, Yamashita N, et al. Cell cycle and apoptosis regulator 1, CCAR1, regulates enhancer-dependent nuclear receptor CAR transactivation. *Mol Pharmacol*. 2019;95(1):120–126. doi:10.1124/mol.118.114272
30. Seo WY, Jeong BC, Yu EJ, et al. CCAR1 Promotes chromatin loading of androgen receptor (AR) transcription complex by stabilizing the association between AR and GATA2. *Nucleic Acids Res*. 2013;41(18):8526–8536. doi:10.1093/nar/gkt644
31. Hosono N. Genetic abnormalities and pathophysiology of MDS. *Int J Clin Oncol*. 2019;24(8):885–892. doi:10.1007/s10147-019-01462-6
32. Visconte V, Nokashima MO, Rogers HJ. Mutations in splicing factor genes in myeloid malignancies: significance and impact on clinical features. *Cancers*. 2019;11(12):1–13. doi:10.3390/cancers11121844
33. Shen W, Szankasi P, Sederberg M, et al. Concurrent detection of targeted copy number variants and mutations using a myeloid malignancy next generation sequencing panel allows comprehensive genetic analysis using a single testing strategy. *Br J Haematol*. 2016;173(1):49–58. doi:10.1111/bjh.13921
34. Hobor F, Dallmann A, Ball NJ, et al. A cryptic RNA-binding domain mediates SYNCRIP recognition and exosomal partitioning of miRNA targets. *Nat Commun*. 2018;9(1):831. doi:10.1038/s41467-018-03182-3
35. Santangelo L, Giurato G, Cicchini C, et al. The RNA-binding protein SYNCRIP Is a component of the hepatocyte exosomal machinery controlling microRNA sorting. *Cell Rep*. 2016;17-(3):799–808. doi:10.1016/j.celrep.2016.09.031
36. Vu LP, Prieto C, Amin EM, et al. Functional screen of MSI2 interactors identifies an essential role for SYNCRIP in myeloid leukemia stem cells. *Nat Genet*. 2017;49(6):866–875. doi:10.1038/ng.3854
37. Martinez FJ, Pratt GA, Van Nostrand EL, et al. Protein-RNA networks regulated by normal and ALS-associated mutant HNRNPA2B1 in the nervous system. *Neuron*. 2016;92(4):780–795. doi:10.1016/j.neuron.2016.09.050
38. Wang H, Liang L, Dong Q, et al. Long noncoding RNA miR503HG, a prognostic indicator, inhibits tumor metastasis by regulating the HNRNPA2B1/NF-kappaB pathway in hepatocellular carcinoma. *Theranostics*. 2018;8(10):2814–2829. doi:10.7150/thno.23012
39. Campa D, Matarazzi M, Greenhalf W, et al. Genetic determinants of telomere length and risk of pancreatic cancer: a pandora study. *Int J Cancer*. 2019;144(6):1275–1283. doi:10.1002/ijc.31928
40. van Maldegem F, Maslen S, Johnson CM, et al. CTNNBL1 facilitates the association of CWC15 with CDC5L and is required to maintain the abundance of the Prp19 spliceosomal complex. *Nucleic Acids Res*. 2015;43(14):7058–7069. doi:10.1093/nar/gkv643
41. Teng H, Wei W, Li Q, et al. Prevalence and architecture of post-transcriptionally impaired synonymous mutations in 8,320 genomes across 22 cancer types. *Nucleic Acids Res*. 2020;48-(3):1192–1205. doi:10.1093/nar/gkaa019
42. Bonnal SC, Lopez-Oreja I, Valcarcel J. Roles and mechanisms of alternative splicing in cancer—implications for care. *Nat Rev Clin Oncol*. 2020;17(8):457–474. doi:10.1038/s41571-020-0350-x
43. Montes M, Sanford BL, Comiskey DF, Chandler DS. RNA splicing and disease: animal models to therapies. *Trends Genet*. 2019;35(1):68–87. doi:10.1016/j.tig.2018.10.002
44. Pellarin I, Belletti B, Baldassarre G. RNA splicing alteration in the response to platinum chemotherapy in ovarian cancer: a possible biomarker and therapeutic target. *Med Res Rev*. 2021;41(1):586–615. doi:10.1002/med.21741